Supplementary Materials for

Achieving Superior Cycling Stability by In-Situ Forming NdH_2-Mg-Mg_2Ni Nanocomposites

Qun Luo, Qinfen Gu, Bin Liu, Teng-Fei Zhang, Wenqing Liu, Qian Li *

* Corresponding author.

E-mail address: shuliqian@shu.edu.cn (Q. Li)

The file includes:

Supplementary Figures

- Figure S1. The comparison of particle sizes of $Nd_{4.3}Mg_{87.0}Ni_{8.7}$ alloy after 38 and 819 H/D cycles
- Figure S2. The SEM images of $Nd_{4.3}Mg_{87.0}Ni_{8.7}$ alloy after different cycles: (a~c) after 38 cycles, (d~h) after 819 cycles with various magnifications
- Figure S3. TEM analysis of fully hydrogenated $Nd_{4.3}Mg_{87.0}Ni_{8.7}$ powder after 38 H/D cycles: (a) bright field TEM micrograph of sample, (b) SAED pattern acquired from the small crystallite cluster indexed as belonging to NdH_2, (c) SAED pattern of dark block indexed as belonging to Mg_2NiH_4, (d) dark field micrograph of NdH_2 obtained using a portion of the (111) ring that is marked in (b)
- Figure S4. (a) The interatomic spacing misfit (f_r) and interplanar spacing misfit (f_d) between different phases, (b) The high resolution TEM image of the NdH_2/Mg and NdH_2/Mg_2Ni interface
- Figure S5. (a) The schematic of a MgH_2/Mg interface after geometry optimization viewing from $[100]_{MgH2}//[0001]_{Mg}$, (b) the optimized structure after a hydrogen atom at the interface diffusing to the nearest neighbor octahedral interstitial, and (c) the

calculated energy changes corresponding to the diffusion path

- Figure S6. The interface structure after geometry optimization with lacking of different layers
- Figure S7. The hydrogenated layer on the surface of sample and the prepared APT specimens

References

Supplementary Figures:

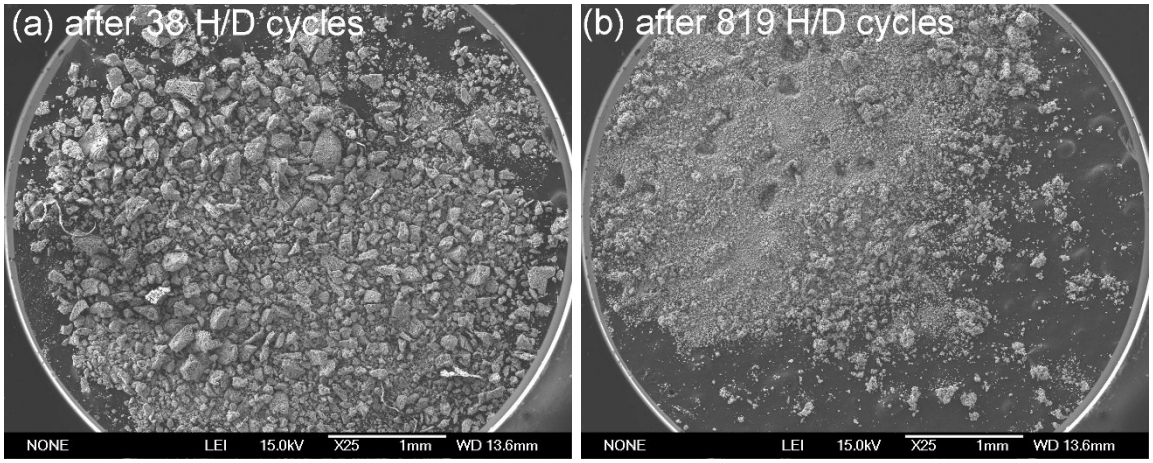

Figure S1. The comparison of particle sizes of $Nd_{4.3}Mg_{87.0}Ni_{8.7}$ alloy after 38 and 819 H/D cycles

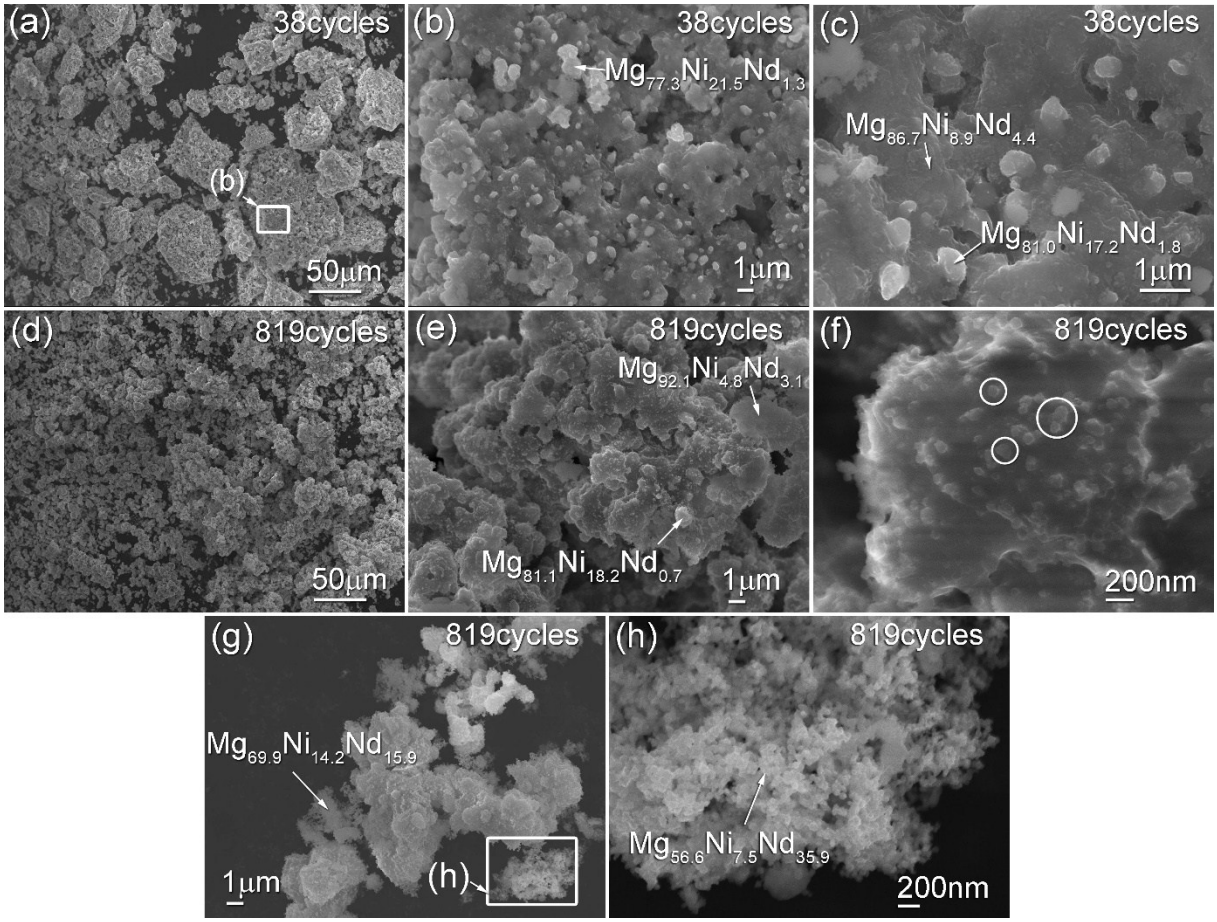

Figure S2. The SEM images of $Nd_{4.3}Mg_{87.0}Ni_{8.7}$ alloy after different cycles: (a~c) after 38 cycles, (d~h) after 819 cycles with various magnifications

Remarks of Figure S1 and S2:

There are many small white particles with diameter less than 1 μm distributed in the samples. The small particles are supposed to be Mg_2Ni as the Ni content in the small particles (17.2~21.5 at.%) is relatively higher than that in the matrix (about 8.9 at.%). After 819 cycles, the uniformly distributed Mg_2Ni particles can still be observed in Figure S2e. However, a large number of nano-particles appear on the surface of powders. Figure S2f shows the high magnification image where the nano-particles are marked by white rings with diameters less than 100 nm. At the other part of sample, we also observe the cluster of the nano-particles and the composition determined by EDS shows much higher Nd content (Figure S2 g and h) than the nominal composition.

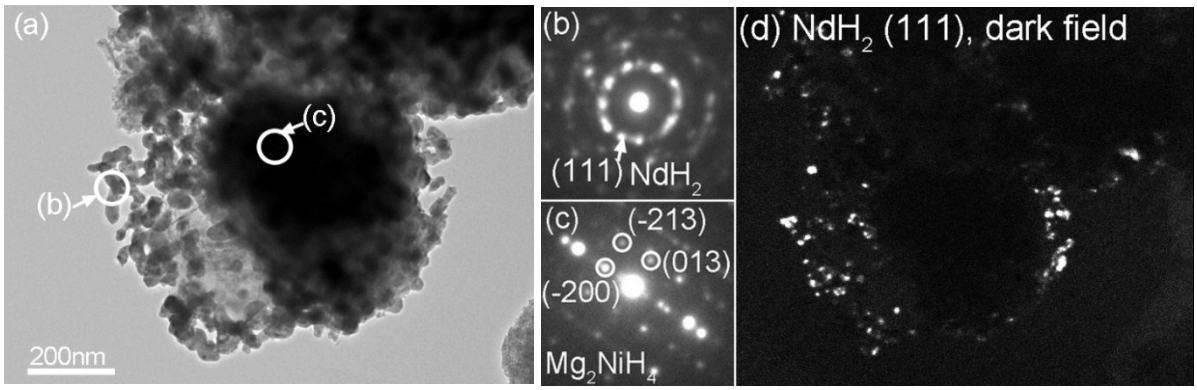

Figure S3. TEM analysis of fully hydrogenated $Nd_{4.3}Mg_{87.0}Ni_{8.7}$ powder after 38 H/D cycles: (a) bright field TEM micrograph of sample, (b) SAED pattern acquired from the small crystallite cluster indexed as belonging to NdH_2, (c) SAED pattern of dark block indexed as belonging to Mg_2NiH_4, (d) dark field micrograph of NdH_2 obtained using a portion of the (111) ring that is marked in (b)

Remarks of Figure S3:

The dark field image of NdH_2 obtained using a portion of the (111) ring illustrates the NdH_2 distribution in the MgH_2 or Mg_2NiH_4 matrix.

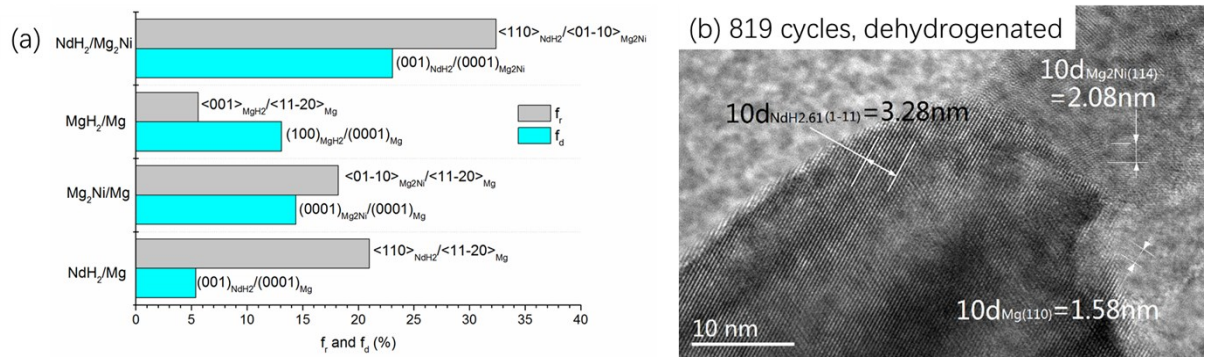

Figure S4. (a) The interatomic spacing misfit (f_r) and interplanar spacing misfit (f_d) between different phases, (b) The high resolution TEM image of the NdH_2/Mg and NdH_2/Mg_2Ni interface

Remarks of Figure S4:

For comparison, Figure S4(a) lists the lowest misfit matching between phases existed in the composites. A good crystallographic matching requires the interatomic spacing misfit along matching direction and interplanar misfit less than 10% and 6%, respectively [1, 2], but the small interatomic spacing misfit is essential. According to this rule, the possible coherent interface only exists between MgH_2/α-Mg and NdH_2/α-Mg. The predicted OR between MgH_2/α-Mg is $[001]_{MgH_2}\left\|[11-20]_{Mg}\right.$ and $(100)_{MgH_2}\left\|(0001)_{Mg}\right.$. Actually, there are three distinct types of OR for the desorption reaction of MgH_2: that of Schober [3] $[001]_{MgH_2}\left\|[11-20]_{Mg}\right.$ and $(100)_{MgH_2}\left\|(0001)_{Mg}\right.$, that of Paik et al. [4] $[001]_{MgH_2}\left\|[-2110]_{Mg}\right.$ and $(-110)_{MgH_2}\left\|(0001)_{Mg}\right.$, and that of Danaie et al. [5] $[-111]_{MgH_2}\left\|[01-11]_{Mg}\right.$ and $(110)_{MgH_2}\left\|(-110-1)_{Mg}\right.$, respectively. The misfits of former two directions are identical. The interatomic spacing misfit in the case of Schober and Paik et al. is less than that of Danaie et al.. In addition, the interplanar misfit between $(100)_{MgH_2}\left\|(0001)_{Mg}\right.$ is less than that of $(-110)_{MgH_2}\left\|(0001)_{Mg}\right.$ ($f_{d,Schober}$=13%, $f_{d,Paik}$=23%). Thus, we choose the Schober type OR, as same as the predicted one, to construct the MgH_2/α-Mg

interface. The predicted interplanar spacing misfit of $(001)_{NdH2} \parallel (0001)_{Mg}$ is less than 6% [1, 2], but the essential interatomic spacing misfit $[110]_{NdH2} \parallel [11\bar{2}0]_{Mg}$ is much larger than the criteria value.

Figure S4(b) shows the interface between NdH_2/α-Mg and NdH_2/Mg_2Ni determined by high resolution TEM. However, it is hardly to observe the orientation relationship (OR) between both interfaces because the grain boundaries of phases are disordered after long-time cycles.

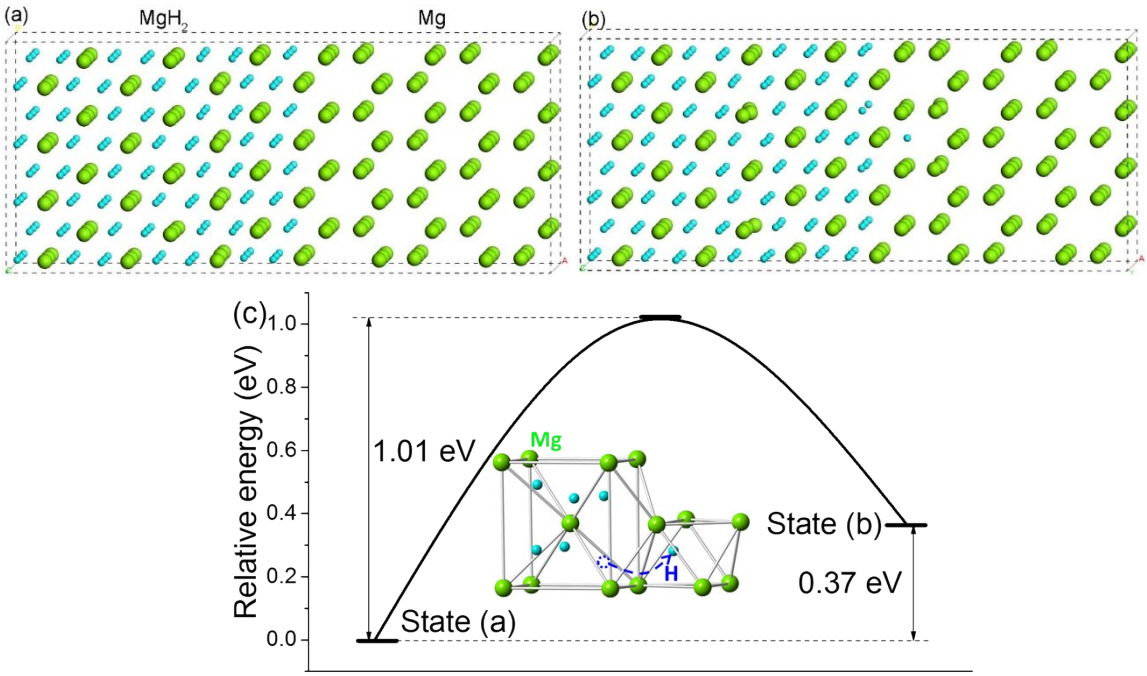

Figure S5. (a) The optimized MgH_2/Mg interface viewing from $[100]_{MgH2}//[0001]_{Mg}$, (b) the optimized structure with hydrogen atom at the interface diffusing to the neighbor octahedral interstitial, and (c) the calculated energy changes corresponding to the diffusion path

Remarks of Figure S5:

With regard to MgH_2/α-Mg interface, a supercell including 360 atoms with size of 29.20×12.34×14.72 $Å^3$ is constructed. After relaxation, the distance between neighboring Mg and H atoms at the interface is reduced from 2.154 to 2.025 Å, which is close to the length of Mg–H bond in MgH_2 [6]. Figures S5 a and b show the optimized structure of the superlattice before and after the hydrogen diffusion. The hydrogen atom at the interface will diffuse to the

nearest neighboring octahedral interstitial in the α-Mg and the diffusion of hydrogen in α-Mg is mainly by jumping from one octahedral interstitial to another [7]. The calculated energy barrier is 1.01 eV for diffusion from state (a) to state (b) (Figure S5c). Furthermore, the system energy increases by 0.37 eV if the reaction occurs. It suggests that the hydrogen atoms prefer to stay in MgH_2 rather than in α-Mg. Therefore, it is difficult for the hydrogen in MgH_2 to diffuse into α-Mg.

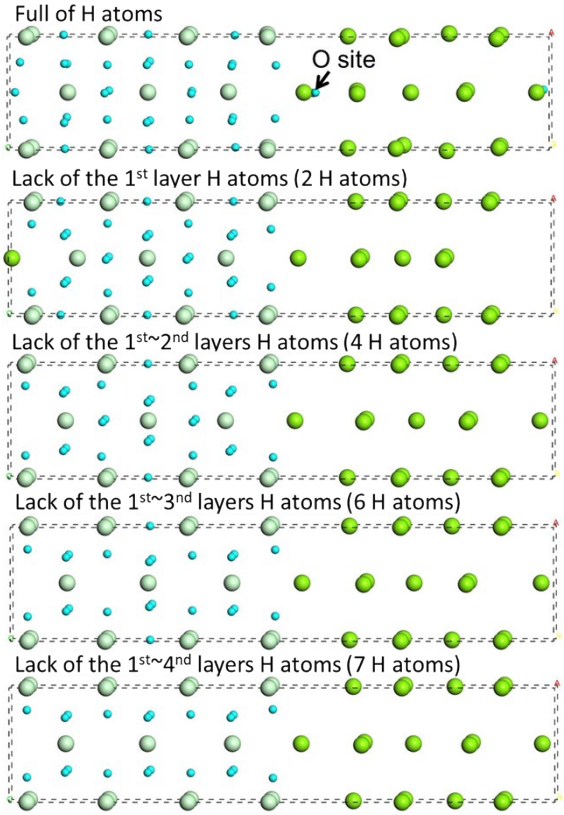

Figure S6. The interface structure after geometry optimization with lacking of different layers of hydrogen

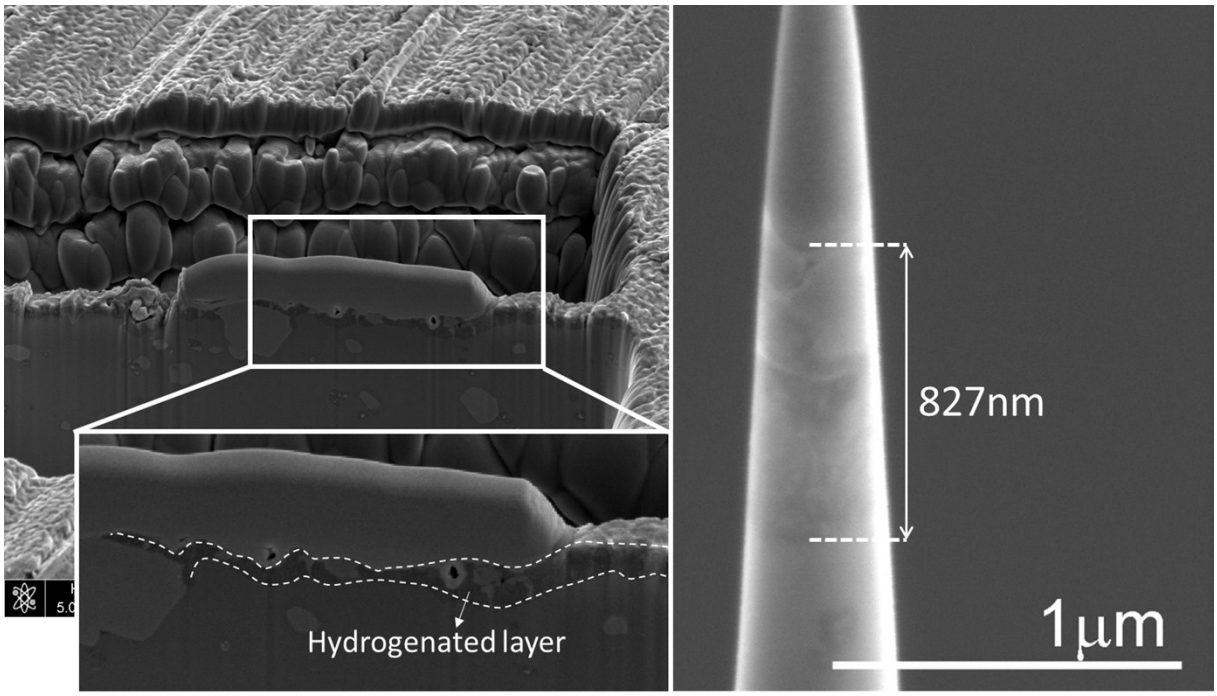

Figure S7. The hydrogenated layer on the surface of sample and the prepared APT specimens

References

1. M. X. Zhang and P. M. Kelly, *Acta Mater.*, 2005, **53**, 1073-1084.

2. P. M. Kelly, H. P. Ren, D. Qiu and M. X. Zhang, *Acta Mater.*, 2010, **58**, 3091-3095.

3. T. Schober, *Metall. Trans. A*, 1981, **12**, 951-957.

4. B. Paik, I. P. Jones, A. Walton, V. Mann, D. Book and I. R. Harris, *Philos. Mag. Lett.*, 2010, **90**, 1-7.

5. M. Danaie and D. Mitlin, *Acta Mater.*, 2012, **60**, 6441-6456.

6. F. H. Ellinger, C. E. J. Holley, B. B. McInteer, D. Pavone, R. M. Potter, E. Staritzky and W. H. Zachariasen, *J. Am. Chem. Soc.*, 1955, **77**, 2647-2648.

7. H. G. Schimmel, G. J. Kearley, J. Huot and F. M. Mulder, *J. Alloys Compd.*, 2005, **404-406**, 235-237.